3.1 Hz; *p*-Ph), 134.0 (d, $^3J(P,C) = 11.2$ Hz; *o*-Ph), 183.6 (dd, $^2J(P,C) = 16.4$ Hz, $^2J(P,C) = 10.7$ Hz; PC*C*N), 198.9 (d, $^2J(P,C) = 7.9$ Hz; *cis*-CO), 202.5 (d, $^2J(P,C) = 23.4$ Hz; *trans*-CO); $^{31}P\{^1H\}$ NMR (81.0 MHz, $CDCl_3$, 25 °C, ext. 85% H_3PO_4): $\delta = 46.4$ (d, $^4J(P,P) = 5.1$ Hz; PPh_2), 159.8 (d, $^1J(W,P) = 260.9$ Hz; PW).

Received: November 9, 2001 [Z18194]

[1] O. I. Kolodiazhni, *Phosphorus-Ylides*, Wiley-VCH, Weinheim, **1999**.
[2] For a discussion of the bonding in **I** and the presentation of its chemical formula see ref. [1].
[3] For examples of other possibile modes of activation, see: a) reductively induced dimerization of benzene ligands in $[\mu^6\text{-}(C_6H_6)Mn(CO)_3]^+$: R. L. Thompson, S. J. Geib, N. J. Cooper, *J. Am. Chem. Soc.* **1991**, *113*, 8961; b) [4+1] self-addition in aryl(arylimino)-phosphanes: E. Niecke, M. Link, M. Nieger, *Chem. Ber.* **1992**, *125*, 2635.
[4] J. C. Baldwin, W. C. Kaska, *Inorg. Chem.* **1979**, *18*, 687.
[5] G. Erker, P. Czisch, R. Benn, A. Rufinska, R. Mynott, *J. Organomet. Chem.* **1987**, *328*, 101.
[6] R. Streubel, H. Wilkens, A. Ostrowski, C. Neumann, F. Ruthe, P. G. Jones, *Angew. Chem.* **1997**, *109*, 1549; *Angew. Chem. Int. Ed. Engl.* **1997**, *36*, 1492.
[7] H. Wilkens, F. Ruthe, P. G. Jones, R. Streubel, *Chem. Eur. J.* **1998**, *4*, 1542.
[8] G. N. Cloke, P. B. Hitchcock, U. Schiemann, R. Streubel, J. F. Nixon, D. J. Wilson, *Chem. Commun.* **2000**, 1659.
[9] R. Streubel, U. Schiemann, N. Hoffmann, Y. Schiemann, P. G. Jones, D. Gudat, *Organometallics* **2000**, *19*, 475.
[10] R. Streubel, U. Schiemann, P. G. Jones, N. H. Tran Huy, F. Mathey, *Angew. Chem.* **2000**, *112*, 3845; *Angew. Chem. Int. Ed.* **2000**, *39*, 3686.
[11] R. Streubel, U. Schiemann, N. H. Tran Huy, F. Mathey, *Eur. J. Inorg. Chem.* **2001**, 3175.
[12] R. Streubel, A. Ostrowski, S. Priemer, U. Rohde, J. Jeske, P. G. Jones, *Eur. J. Inorg. Chem.* **1998**, 257.
[13] H. J. Bestmann, M. Schmidt, *Angew. Chem.* **1987**, *99*, 64; *Angew. Chem. Int. Ed. Engl.* **1987**, *26*, 79.
[14] R. Streubel, N. Hoffmann, unpublished results.
[15] M. J. van Eis, C. M. D. Komen, F. J. J. de Kanter, W. H. de Wolf, K. Lammertsma, F. Bickelhaupt, M. Lutz, A. L. Spek, *Angew. Chem.* **1998**, *110*, 1656; *Angew. Chem. Int. Ed.* **1998**, *37*, 1547.
[16] F. Bickelhaupt, W. H. de Wolf, *Adv. Strain. Org. Chem.* **1993**, *3*, 185.
[17] M. Schiffer, M. Scheer, *Angew. Chem.* **2001**, *113*, 3520; *Angew. Chem. Int. Ed.* **2001**, *40*, 3413.
[18] **5**: MS (positive-ion FAB (nitrobenzyl alcohol), ^{184}W): *m*/*z* (%) 888 (20) $[M+H]^+$, the isotope pattern is in agreement with calculation.
[19] Crystal structure of complex **5** ($C_{35}H_{43}NO_5P_2Si_3W$): triclinic, space group $P\bar{1}$, $a = 10.9277(12)$, $b = 13.3245(16)$, $c = 13.7618(16)$ Å, $\alpha = 90.325(6)$, $\beta = 91.388(6)$, $\gamma = 103.281(6)°$, $V = 1934.9$ Å^3, $Z = 2$, $\mu = 5.0$ mm^{-1}, $T = -140$ °C. A yellow tablet with dimensions of about $0.1 \times 0.1 \times 0.03$ mm was mounted in perfluoropolyether oil on a Bruker SMART 1000 CCD diffractometer. Intensity data were registered to $2\theta_{max} = 52°$ ($Mo_{K\alpha}$). Of a total of 24130 reflections, 7889 were independent ($R_{int} = 0.073$). After a semiempirical absorption correction (SADABS), the structure was solved with the heavy-atom method and refined anisotropically against F^2 (program SHELXL-97, G. M. Sheldrick, University of Göttingen. Hydrogen atoms were included by using a riding model or as rigid methyl groups. Final *wR*2 (all data) = 0.0808, conventional $R1 = 0.042$, 433 parameters; $S = 0.922$; max. $\Delta\rho = 1.861/-1.953$ e Å^{-3}. CCDC-173084 contains the supplementary crystallographic data for this paper. These data can be obtained free of charge via www.ccdc.cam.ac.uk/conts/retrieving.html (or from the Cambridge Crystallographic Data Centre, 12, Union Road, Cambridge CB2 1EZ, UK; fax: (+44) 1223-336-033; or deposit@ccdc.cam.ac.uk).
[20] R. Streubel, H. Wilkens, P. G. Jones, *Chem. Eur. J.* **2000**, *6*, 3997.
[21] H. Wilkens, Dissertation, Technische Universität Braunschweig, **2000**.
[22] F. A. Allen, O. Kennard, D. G. Watson, L. Brammer, A. G. Orpen, R. Taylor, *J. Chem. Soc. Perkin Trans. 2* **1987**, S1.

Self-Assembly of ZnO: From Nanodots to Nanorods**

Claudia Pacholski, Andreas Kornowski, and Horst Weller*

Bottom-up techniques for the fabrication of small particles, which mostly arise from colloid chemistry, are integral components in nanotechnology and materials manufacturing. Control of particle size, shape, and crystalline structure represent some of the key issues in this area. Classical models describe the genesis of particles by the formation of tiny crystalline nuclei in a supersaturated medium followed by crystal growth. The latter process is controlled by mass transport and by the surface equilibrium of addition and removal of individual monomers, that is atoms, ions, or molecules. Hereby, the driving force for monomer removal (dissolution) increases with decreasing particle size. Thus, within an ensemble of particles with slightly different sizes the large particles will grow at the cost of the small ones. This mechanism is called Ostwald ripening and is generally believed to be the main path of crystal growth.

A different view of crystal growth is emerging from recent experiments by Penn and Banfield.[1–3] They observed that anatase and iron oxide nanoparticles with sizes of a few nm can coalesce under hydrothermal conditions in a way they call "oriented attachment". In the so formed aggregates, the crystalline lattice planes may be almost perfectly aligned or dislocations at the contact areas between the adjacent particles lead to defects in the finally formed bulk crystals. They presented strong evidence that this type of crystal growth plays an important role in earth history during mineral formation. Oriented attachment was also proposed by other authors during crystal growth of TiO_2[4] and for micrometer-sized ZnO particles during the formation of rodlike ZnO microcystals.[5] The latter experiments give, however, only indirect evidence.

Self-assembly of colloidal particles into larger aggregates is not principally new. The formation of secondary particles with typical sizes in the micrometer regime is a well-known phenomenon in classic colloid chemistry.[6] Kinetic models for this type of growth have been developed which do, however, not consider the process on an atomic level nor give attention to crystallographic orientation of the aggregated particles. Indeed, the X-ray diffraction (XRD) pattern of those secondary particles usually indicate polycrystalline morphology.

Recently, self-assembly of ligand-stabilized nanoparticles with sizes of a few nanometer into two- and three-dimen-

[*] Prof. Dr. H. Weller, C. Pacholski, Dipl.-Ing. A. Kornowski
Institut für Physikalische Chemie
Universität Hamburg
Bundesstrasse 45, 20146 Hamburg (Germany)
Fax: (+49) 40-42838-3452
E-mail: weller@chemie.uni-hamburg.de

[**] We thank Philips Analytical and J. Kolny for X-ray diffraction measurements.

Supporting information for this article is available on the WWW under http://www.angewandte.com or from the author.

sionally ordered arrays has been reported.[7] In these experiments, however, self-assembly is mainly driven by the interactions of the organic ligands rather than by the interaction of the particle cores. Contrarily self-assembled "oriented attachment" was only observed for ligand-free nanoparticles.

Recently, rodlike semiconductor and metal nanoparticles have attracted considerable attention. There are, however, only a few examples reported where those nanorods could be prepared in a controllable manner using evaporation or colloido-chemical techniques.[8–14] Materials such as ZnO, Co, Au, and CdSe were used for the rods. Rod formation requires anisotropic crystal growth which is usually realized when the free surface energies of the various crystallographic planes differ significantly. For wet chemical synthesis Puntes et al. recently showed that this could be realized in the case of CdSe and Co[15] by using two different surface ligands, which probably bind selectively to the respective surface planes.

We report here the formation of high-quality single crystalline ZnO nanorods which is based on oriented attachment of preformed quasi-spherical ZnO nanoparticles. The growth from individual particles by crystallographically oriented and partially fused dimers and oligomers to almost perfect rods is monitored by high-resolution transmission electron microscopy (TEM) and XRD.

ZnO nanoparticles were prepared from zinc acetate dihydrate in alcoholic solution under basic conditions.[16] The procedure is a modification of the method developed by Henglein et al.[17] We found that the shape of the ZnO particles was very sensitive to the overall concentration of precursors. At a zinc acetate dihydrate concentration of below 0.01 M quasi-spherical particles were formed, whereas mainly nanorods were formed at 10 times higher concentrations. Similar observations were reported by Vergés et al. for the formation of rodlike microcrystals.[5]

To learn more about the growth mechanism, we have performed the experiments in a different way. We first prepared a sol of quasi-spherical particles at low concentrations (0.01 M, starting sol), increased the particle concentration in a second step by solvent evaporation, and finally refluxed these colloidal solutions for different lengths of time. Rod formation occurred exclusively during the final heating step, that is from already formed quasi-spherical particles. All experiments described in hereafter were performed under these conditions. The particles of the starting sol are depicted in the TEM image in Figure 1 A. An average particle size of approximately 3 nm is seen and it is assumed that facetted crystalline surfaces are already present, but not detectable by high-resolution TEM due to the small size and relatively low contrast of ZnO. The corresponding powder X-ray diffractogram is depicted in Figure 2 (curve A). It exhibits the typical size-broadened reflections from wurtzite-type ZnO. Scherrer line width analysis of all shown peaks yields particle diameters around 3 nm which is consistent with the TEM images. Increasing the particle concentration by a factor of 10 by evaporation of the solvent at room temperature resulted in a particle growth from 3 nm to 5 nm without, however, changing the shape of the particles. The same effect was observed after reflux of the starting sol for 8 h before the concentration step. Such a gradual growth of quasi-spherical ZnO particles upon aging was also observed and explained by Ostwald ripening.[18, 19] Refluxing, however, the concentrated solution yields rodlike nanoparticles. An increase in the heating time mainly leads to an increase of the elongation of the particle

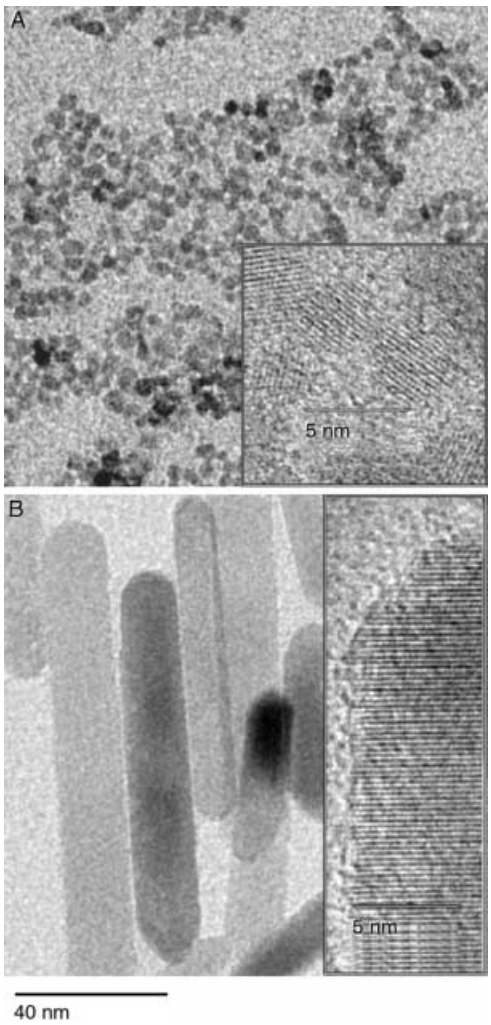

Figure 1. TEM images of ZnO. A) starting sol; B) after one day of reflux of the concentrated sol. The insets show high-resolution TEM images of individual nanoparticles.

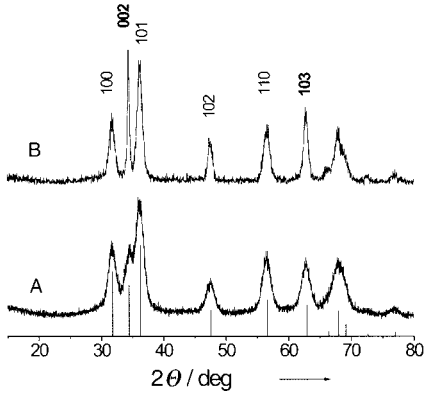

Figure 2. X-ray diffractogram of the ZnO starting sol (A) and after one day of reflux (B).

  1433-7851/02/4107-1189 $ 20.00+.50/0

along the *c* axis. After refluxing for one day, single crystalline nanorods with average lengths of 100 nm and widths of approximately 15 nm were formed (Figure 1 B).[20] In the corresponding XRD image (curve B, Figure 2) the 002 reflection has strongly sharpened up which is consistent with rod formation along the *c* axis. More details about the XRD investigations including solution XRD measurements and simulations are given in the Supporting Information.

Detailed TEM investigations in an early stage of rod formation (reflux for 2 h) are shown in Figure 3. At low magnification (Figure 3 A) aggregated quasi-spherical particles are recognized beside already formed short rods. Most of the aggregated particles form pearl-chain-like structures. High-resolution TEM images of a series of aggregated particles are shown in Figure 3 B – D. It is seen that the lattice planes of the depicted particles are almost perfectly aligned. Moreover, one recognizes that the lattice planes go straight through the contact areas, that is the particles are epitaxially fused together; bottlenecks between the adjacent particles are still visible. In the majority of images we see oriented attachment along the *c* axis (002), but we also find examples of lateral oriented attachment parallel to the *c* axis. In some cases one can even observe how the individual particles are aligned like a wall, where the second layer of bricks is just started to be put on the first (Figure 3 E). The observed lattice planes in these images are the 002 or 100, which lie perpendicular or parallel to the *c* axis, respectively. In all images the longest extension of the aggregates is manifested in the direction of the *c* axis. More examples are shown in the Supporting Information. We do not observe oriented attachment in all aggregated particles. If, however, the particles are fused together, the lattice planes are aligned relative to each other. Thus, oriented attachment seems to be the prerequisite for the condensation step leading to crystallite fusion under our experimental conditions.

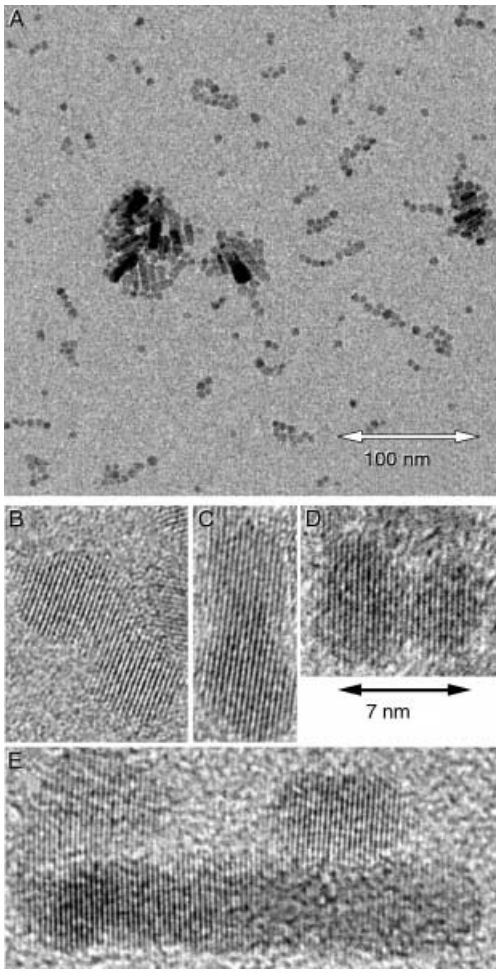

Figure 3. A) TEM image of the concentrated solution after reflux for 2 h; B) – D) high-resolution TEM images of dimers formed by oriented attachment; E) oligomer structure of several nanoparticles fused after oriented attachment.

This type of oriented attachment implies that the aspect ratio of the rods should peak at integer numbers, at least in an early stage of growth, where the width of the rods is almost identical to the diameter of the particles in the concentrated starting sol. This is indeed observed as shown in the histogram in Figure 4.[21]

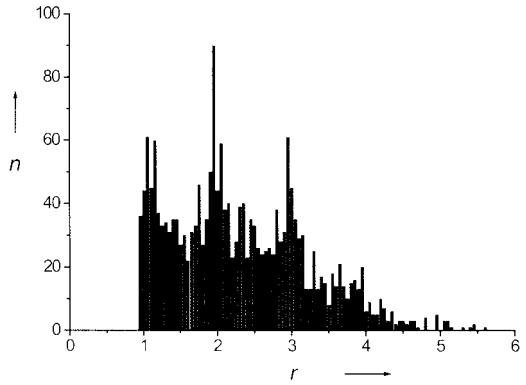

Figure 4. Histogram (with n = frequency) showing the aspect ratio r (length/width) of 2000 ZnO nanorods at an early stage of growth (2 h reflux). The width of the rods at this stage is almost identical to the diameter of the quasi-spherical nanoparticles.

In summary the presented experiments provide strong evidence that oriented attachment of preformed quasi-spherical ZnO nanoparticles is a major reaction path during the formation of single crystalline nanorods under the described conditions. In the finally formed rods the bottlenecks between the adjacent particles must have been filled up and the surfaces parallel to the *c* axis must somehow have been smoothened. We believe that this occurs by conventional mechanism of dissolution and growth of monomers, which might also result in an overall growth of the rods, especially after long times of reflux. In this sense, Ostwald ripening does not only compete with, but assists the growth process by oriented attachment in order to yield finally high-quality rodlike nanocrystals.

Presently we can only speculate why oriented attachment preferentially occurs along the *c* axis (although it also happens along other crystal orientations). One reason might arise from the wurtzite structure itself. If complete 002 planes are formed, their reactivity should be different at the bottom and the top of the *c* axis, since one of these layers is formed by zinc

  1433-7851/02/4107-1190 $ 20.00+.50/0

and the other by oxygen. In alkaline water-containing solutions, this situation will partially be altered by the adsorption of OH^- or H_2O. Zn and O atoms are located in an alternating manner in the 100 planes parallel to the *c* axis. Thus, hydroxylation and therefore also counterion adsorption should be different. Different amounts of counterions or different surface charges could hinder or favor oriented attachment which requires an intimate contact of the respective surface planes. Also the acetate ions from the precursor salt might act in this sense. A similar role of counterion adsorption is currently also discussed for crystal growth during biomineralization.[22]

We believe that oxide nanoparticles are very favorable for oriented attachment for two reasons: first, organic ligands, which prevent intimate contact of crystal planes, are usually not needed for stabilization; and second, crystalline fusion of correctly attached particles does not only lead to a gain in lattice-free energy but also in free energy of polycondensation.

The presented growth mechanism offers an excellent tool to design advanced materials with anisotropic materials properties. One application is the inclusion of nanoparticle building blocks with a large number of reactive surfaces—a situation that is already partially realized with the growth of ZnO nanoparticles (cf. Figure 3E). This would open access to the synthesis of more complex crystalline three-dimensional structures in which the branching sites could be added as individual nanoparticles.

Experimental Section

For the preparation of the ZnO nanospheres zinc acetate dihydrate (0.01 M) was dissolved in methanol (125 mL) under vigorous stirring at about 60 °C. Subsequently, a 0.03 M solution of KOH (65 mL) in methanol was added dropwise at 60 °C. The reaction mixture was stirred for 2 h at 60 °C (details see ref. [16]). The resulting solution (stock solution) was concentrated by evaporation of the solvent and heated for different lengths of time to obtain rod-shaped particles.

Received: January 10, 2002 [Z18502]

[1] J. F. Banfield, S. A. Welch, H. Zhang, T. T. Ebert, R. L. Penn, *Science* **2000**, *289*, 751 – 754.
[2] R. L. Penn, J. F. Banfield, *Science* **1998**, *281*, 969 – 971.
[3] R. L. Penn, J. F. Banfield, *Geochim. Cosmochim. Acta* **1999**, *63*, 1549 – 1557.
[4] A. Chemseddine, T. Moritz, *Eur. J. Inorg. Chem.* **1999**, 235 – 245.
[5] M. A. Verges, A. Mifsud, C. J. Serna, *J. Chem. Soc. Faraday Trans.* **1990**, *86*, 959 – 963.
[6] J. Park, V. Privman, E. Matijevic, *J. Phys. Chem. B* **2001**, *105*, 11630 – 11635.
[7] C. P. Collier, T. Vossmeyer, J. R. Heath, *Annu. Rev. Phys. Chem.* **1998**, *49*, 371 – 404.
[8] W. Han, S. Fan, Q. Li, Y. Hu, *Science* **1997**, *277*, 1287 – 1289.
[9] A. M. Morales, C. M. Lieber, *Science* **1998**, *279*, 208 – 211.
[10] Y. Li, G. W. Meng, L. D. Zhang, F. Phillipp, *Appl. Phys. Lett.* **2000**, *76*, 2011 – 2013.
[11] S. Link, Z. L. Wang, M. A. El-Sayed, *J. Phys. Chem. B* **2000**, *104*, 7867 – 7870.
[12] X. Peng, L. Manna, W. Yang, J. Wickham, E. Scher, A. Kadavanich, A. P. Alivisatos, *Nature* **2000**, *404*, 59 – 61.
[13] L. Guo, S. Yang, C. Yang, P. Yu, J. Wang, W. Ge, G. K. L. Wong, *Chem. Mater.* **2000**, *12*, 2268 – 2274.
[14] K. Kamata, H. Hosono, Y. Maeda, K. Miyokawa, *Chem. Lett.* **1984**, 2021 – 2022.
[15] V. F. Puntes, K. M. Krishnan, A. P. Alivisatos, *Science* **2001**, *291*, 2115 – 2117.
[16] H. Womelsdorf, W. Hoheisel, G. Passing, DE-A 199 07 704 A 1, **2000**.
[17] M. Haase, H. Weller, A. Henglein, *J. Phys. Chem.* **1988**, *92*, 482 – 487.
[18] E. A. Meulenkamp, *J. Phys. Chem. B* **1998**, 5566 – 5572.
[19] L. Spanhel, M. A. Anderson, *J. Am. Chem. Soc.* **1991**, *113*, 2826 – 2833.
[20] The length of the nanorods could further be increased up to 500 nm by refluxing the solution for several days.
[21] To ensure a statistical significance, we have investigated 2000 particles. The shape of the histogram is also not sensitive to the number of data bars.
[22] S. Rajam, S. Mann, *J. Chem. Soc. Chem. Commun.* **1990**, 1789.

  1433-7851/02/4107-1191 $ 20.00+.50/0